Sensors International 2 (2021) 100128

Contents lists available at ScienceDirect

Sensors International

journal homepage: www.keaipublishing.com/en/journals/sensors-international

An artificial neural network based detection and classification of melanoma skin cancer using hybrid texture features

Priyanti Paul Tumpa *, Md Ahasan Kabir

Department of Electronics and Telecommunication Engineering, Chittagong University of Engineering and Technology, Chattogram, Bangladesh

ARTICLE INFO

Keywords:
Maximum gradient intensity
Skin cancer
Hybrid texture features
Malignant

ABSTRACT

Melanoma being the most unpredictable and life-threating cancer, has been on the rise in recent times. In most of the cases being fatal, if treated early, the fatality rate might be lowered severely. Hands-on Melanoma detection at primary stages with the unassisted eye is error-prone and requires vast knowledge and experience. Number of expert dermatologists being inadequate, a computerized and automated approach is needed to accurately detect Melanoma. The following study tries to achieve this feat by developing a neural network that can effectively detect and classify Melanoma. The process begins with preprocessing of dermoscopic images to remove hairs with the Maximum Gradient Intensity algorithm and also enhancement of the images is done. Segmentation based on Otsu Thresholding algorithm is applied to separate skin lesions from the images. Multiple features like ABCD, GLCM, and LBP are then calculated from the segmented images which will be used to train a neural network. The network was successful to attain an accuracy of 97.7% on the combined dataset of ISIC archive the PH2 dermoscopic image database. The proposed method was found to be more accurate than existing methods and encorporates much more feature information from the images.

1. Introduction

The skin on the body provides a shield of protection against electronic, chemical, and physical injuries. It defends us from diseases and pollutants, avoids moisture loss due to the presence of intercellular lipids in their hydrophilic area that captures water molecules. Because of the pigment melanin which absorbs UV radiation, the skin has the ability to reduce the harmful effects of ultraviolet (UV) radiation. The skin comprises three types of layers known as epidermis, dermis, and hypodermis. The outermost layer, epidermis shields the skin from the surroundings. Underneath the epidermis, there's a layer known as the dermis that includes strong connective tissue and glands of sweat. The hypodermis is a subcutaneous layer that lies beneath the dermis and is mostly made up of fat. Unique cells in the epidermis called melanocytes form the color of the skin and generate the pigment melanin [1,2].

Skin cancers are tumors that grow out of the skin. They are triggered by the production of irregular cells and may infiltrate to certain areas on the human body. Skin cancer is categorized into three types: basal-cell cancer (BCC), squamous-cell cancer (SCC), and melanoma [3]. BCC and SCC are mild skin cancers. The most dangerous one is melanoma. Symptoms include a mole that has evolved in scale, form, color, uneven borders, more than one shade, becomes itchy, or bleeds. In 2018, there were 287,723 new cases of melanoma recorded globally, and the number of deaths due to melanoma was 60,712. In 2019, nearly 96,480 melanomas have been reported in the US, and around 7230 people have died of melanoma (nearly 4740 males and 2490 females) [4]. The main environmental source of skin cancer is ultraviolet radiation from the suns' exposure. Malignant melanoma starts spreading throughout its environment. Although the risk of incidence of melanoma is very significant, but with proper diagnosis at its preliminary condition, the possibility of survival is nearly 100%. As well as being a challenging field of research, melanoma detection and classification in its early phases are also quite essential [4].

Visual imaging for skin cancer diagnosis by medical professionals

* Corresponding author.
E-mail address: u1508003@student.cuet.ac.bd (P.P. Tumpa).

Production and hosting by Elsevier

https://doi.org/10.1016/j.sintl.2021.100128
Received 5 August 2021; Received in revised form 21 September 2021; Accepted 23 September 2021
Available online 30 September 2021

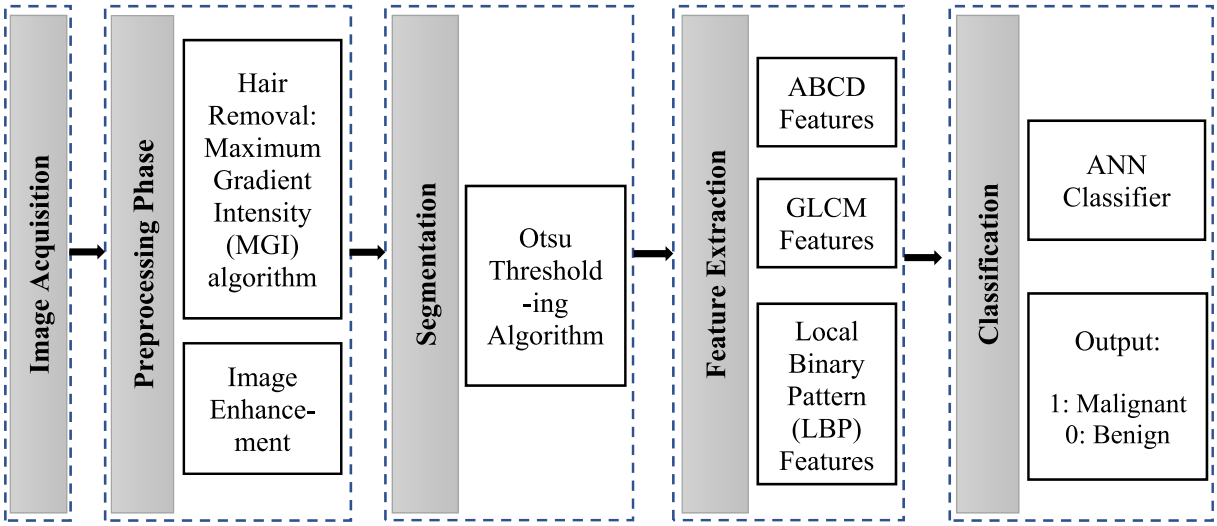

Fig. 1. Flow diagram of the proposed approach to classify melanoma.

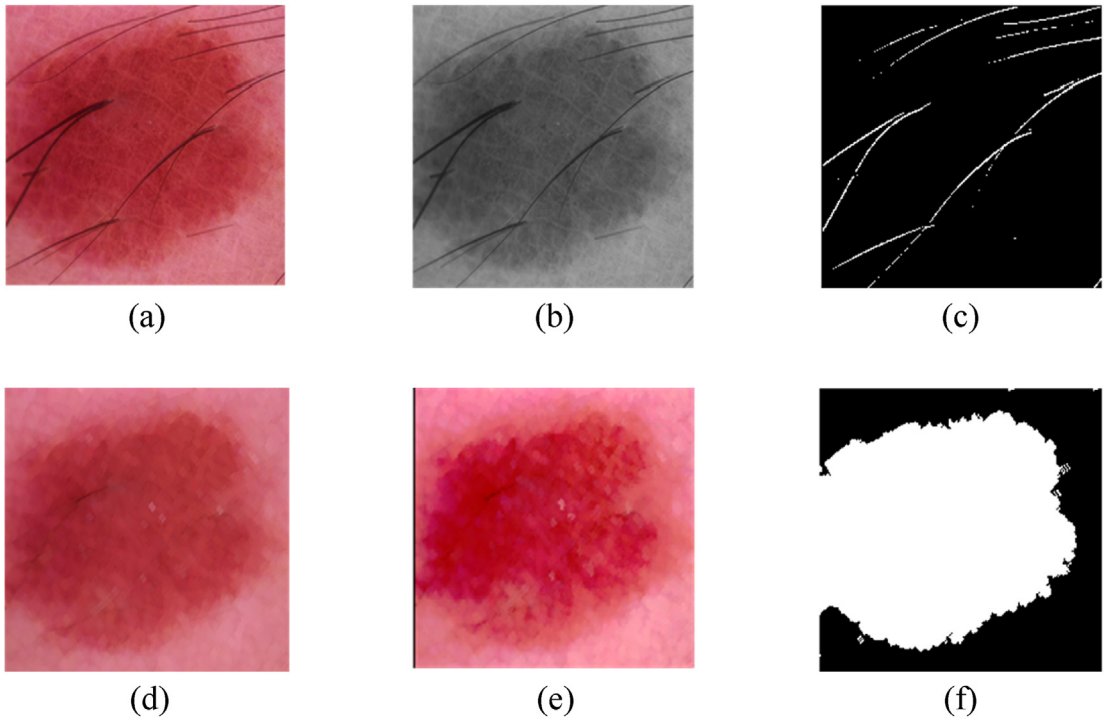

Fig. 2. (a) Input image. (b) Grayscale image. (c) Hair mask containing hair pixels. (d) Image after hair removal with MGI algorithm. (e) Enhanced image (f) Segmented skin lesion.

may not guarantee 100% recognition of malignant or benign cancers. Therefore, automatic classification systems for the detection and classification of skin cancers are urgently needed, which can be accurate and successful [5]. Among the existing clinical methods for melanoma detection, the very first dermoscopic technique for the treatment of melanoma was pattern analysis. Benign and malignant melanoma has their patterns that are discriminated against by color, architecture, symmetry, and homogeneity. ABCD law is a common method of extraction of the feature that lets dermatologists detect melanoma at its early stages. ABCD defines the clinical characteristics of melanoma using the following parameters: Asymmetry Index (A), Border Irregularity (B), Color score (C), and Diameter (D). A malignant lesion is not symmetric in its shape, has irregular borders, more than one color and also it has a diameter of more than 6 mm. Another clinical approach is the 7-point checklist. It has three primary features: an abnormal pigment network, gray-blue patches, and an abnormal vascular arrangement, as well as four minor features: irregular spots, streaks, blotches and evidence of regression. When a melanocytic lesion identifies some of the primary features, urgent assistance from health care professionals is required [6].

Utilizing artificial intelligence coupled with image processing is a very effective technique for classifying malignant and benign skin cancers. Researchers had developed several automatic detection systems to make clinical melanoma treatment less subjective and difficult. Nadia S. and Souhir B [7]. in their paper, presented a digital diagnostic technique based on a combination of the ABCD rule and the region-growing segmentation technique for early melanoma identification. Michal K. et al. [8] in their paper, used an SVM classifier to differentiate between melanoma and other non-melanoma cancers. They also used various

Table 1
Formulas for calculating different GLCM features [20].

Features	Details	Formula
Contrast	Calculates the textural roughness among a pixel and its neighbors throughout the whole picture.	$\sum_{i=1}^{N}\sum_{j=1}^{N}(i-j)^2 P_{i,j}$
Correlation	Assesses the textural homogeneity in between 0 and 1.	$\sum_{i=1}^{N}\sum_{j=1}^{N}\frac{(i,j)(P_{i,j}-\mu_i\mu_j)}{\sigma_x\sigma_y}$
Energy	Quantifies the level of disturbance or non-homogeneity.	$\sum_{i=1}^{N}\sum_{j=1}^{N}P_{i,j}^2$
Homogeneity	Relates to the impact of a pixel's surroundings on the entire picture.	$\sum_{i=1}^{N}\sum_{j=1}^{N}\frac{P_{i,j}}{1+(i-j)^2}$

descriptors which are helpful for pattern recognition in the end. In Ref. [9], a computerized method was developed for the detection of melanoma using different image processing tools. These image processing techniques look for different types of melanoma texture, size, and shape parameters. These different features were used to classify the given skin samples as having melanoma or not.

Another work in Ref. [10] a computer-assisted melanoma detection system involves the acquisition of dermoscopic images, removing noises; segmentation based on Maximum Entropy Thresholding; feature collection using Gray Level Co-occurrence Matrix (GLCM) and classification using Artificial Neural Network (ANN). Deshpande A. S. et al. [11] developed a simple detection and diagnosis system that can be used by non-experts/clinicians/doctors. In their method, images were first pre-processed by using a median filter for removing noises and then segmented through the use of Fuzzy C-Means (FCM), and statistical texture features were extracted using the GLCM. Finally, a Support Vector Machine (SVM) was applied to detect skin cancer or skin allergy. Ganster H [12]. presented a melanoma recognition scheme that involves KNN classifier. The work in Ref. [13] presents an automated image processing system that adds the contextual information like skin type, gender, age with the classifier outputs for reliable classification. Garnavi R. and Aldeen M [14]. in their paper, developed a method that employs boundary and wavelet-based texture features and four distinct classifiers like decision trees, logistic regression, ANN, and SVM in the diagnosis of melanoma. Mazumder S [15]. in their paper, segmented the skin lesion using Otsu's method, then applied the ABCD rule to extract the features. Finally, With the features extracted from 200 images, a Back-propagation Neural Network model is developed. Hairs on the skin can mislead the classification of malignant and benign skin lesions. E-shaver [16] is an efficacious hair occlusion process used on images of the skin that operates on the basis of Radon transform. Lee et al. [17] created the Dull-Razor algorithm to eliminate dark hair from the images. A generic grayscale morphological closure process determines the dark hair pixels and those pixels are replaced by using bilinear interpolation. After that, it smooths the image with the use of a median filter. For this, the image gets blurred and some of its features can get miscalculated. All of these works are able to classify malignant and benign skin lesions but none of them are fully accurate. So, there's a scope of improvement to skin cancer detection and classification method.

In this research, a Maximum Gradient Intensity (MGI) algorithm is developed to detect hair pixels. To increase the system's accuracy, multiple shape and texture features are obtained. The artificial neural network classifier has been successfully trained to distinguish between malignant and benign skin cancer. The outcomes of the network are satisfactory on basis of accuracy, sensitivity, specificity, and precision.

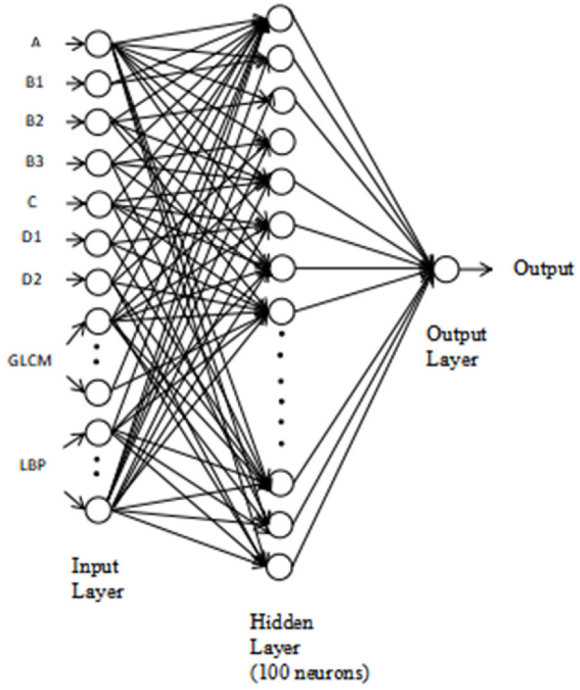

Fig. 3. Structure of the artificial neural network.

Table 3
Malignant and Benign skin lesion classification.

	Actual Benign	Actual Malignant
Predicted Benign	TN = 1902	FP = 41
Predicted Malignant	FN = 38	TP = 1407

2. Proposed approach

Fig. 1 presents the proposed methodology's flow diagram of detecting and classifying melanoma skin lesions, both benign and malignant. It

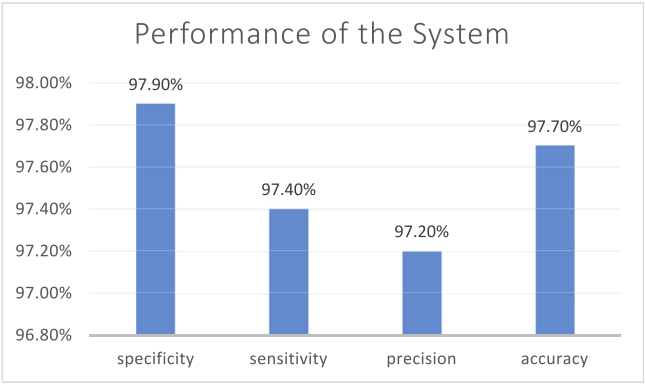

Fig. 4. Performance of the proposed system.

Table 2
Some extracted features from the skin lesion.

Features	A	B1	B2	B3	C	D1	**D2**
Skin lesion	1.01	34.95	0.5117	2.44e+06	1	96.62	2.0848
Features	Contrast	Correlation	Homogeneity	Entropy	Mean	Standard Deviation	
Skin lesion	0.0153	0.9752	0.994	0.5033	0.05848	0.4928	

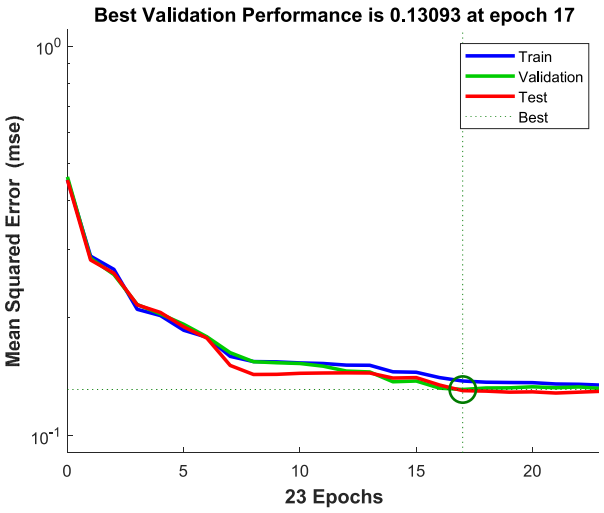

Fig. 5. Mean Squared Error (MSE) curve.

includes image acquisition, image pre-processing, segmentation, extraction of features, and classification technique which are the key steps.

Input Images are collected from two datasets to train the network with more data. The Maximum Gradient Intensity (MGI) algorithm is applied on the image to get rid of the hair artifacts and then the image is enhanced with image enhancement tools. The skin lesion from the image is segmented using an Otsu global thresholding algorithm. From the skin lesions, all types of texture, shape, and color features are extracted and provided to the network for further classification.

2.1. Image acquisition

For successful implementation of the next steps and eventually development of a reliable automated detection approach for melanoma lesions, a suitable input set of data must be collected. In this work, the melanoma classification system used images obtained via dermoscopy. The input images are obtained from the ISIC archive dataset and PH2 dataset. In the ISIC dataset [19], images are captured in the JPEG format with a resolution of 224 by 224 pixels. The data set contains nearly 3600 images of malignant and benign lesions, with both training and testing data. In the PH2 dataset, there are a total of 200 (160 benign and 40 malignant) images in BMP file format with a resolution of 768 by 560 pixels. This dataset was generated through a collaborative research partnership between the University of Portland and the Pedro Hispano Hospital's Dermatology Service in Portugal [18]. The acquired images are in RGB format. Images from two datasets are combined so that training the network with more samples is achieved.

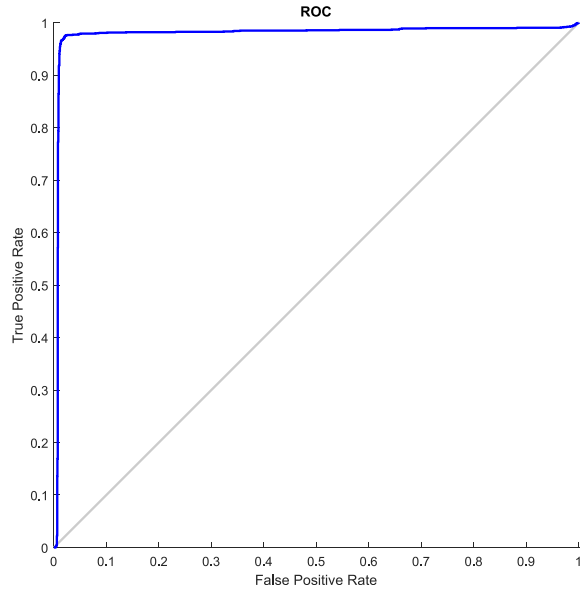

Fig. 6. ROC curve.

2.2. Image preprocessing

Preprocessing is a step that is carried out before processing to fix images for various errors. Input images are obtained from multiple sources, so it is important to translate them to a standard size, standard color and eliminate any unnecessary detail including noise, bubbles, hair, etc. At first, Grayscale transformation is applied to convert input RGB images to grayscale images. A grayscale image is just one in which shades of gray are the only colors and no red, green, or blue is present. Grayscale images simplify image processing operations and reduce complexity.

On the skin, there are hairs which protect the whole body and have a wide range of colors, shapes, and orientations. As a consequence, these hairs will occlude images and lesions, and interrupt the algorithms used to identify lesions. A new Maximum Gradient Intensity (MGI) algorithm is proposed to detect the hair pixels and remove them. The steps of this algorithm are given below:

Step 1: The grayscale image of the input image is created.
Step 2: Horizontal (H_r), Vertical (V_r), and Diagonal (D_u, D_d) intensities are calculated for individual pixel.
Step 3: A new image (hair mask) is generated using

$$i(x,y) = \max(H_r, V_r, D_u, D_d) \quad (1)$$

Step 4: Hair pixel is replaced from the original image by morphological operation (dilation).

After removing the hair artifacts from the image, image enhancement tools are applied to change the image and to bring out image information. It is the process of adjusting digital images to make the results better suited for further analysis of the images. It makes identifying the key features easy. The image is enhanced using the histogram equalization process which increases the contrast of the image.

2.3. Image segmentation

Segmentation's main focus is on finding identical regions within an image and to divide objects into distinct regions based on a threshold value. One of the most effective image segmentation methods is Otsu's Thresholding. It's one of the histogram-based methods for global thresholding. Based on a bi-modal histogram, the technique assumes that the image comprises two categories of pixels (foreground and background) and determines the best threshold for dividing the two classes such that their inter-class variance is largest, or equivalently their intra-class variance is smallest. Otsu's Threshold is a nonlinear method of transforming a gray image to a binary one. The largest segmented object is selected for further analysis and small objects are removed to avoid imprecise analysis.

An image in Fig. 2(a) is chosen as input to visually understand the preprocessing and segmentation stage of this work. Grayscale conversion of input image is represented in Fig. 2(b). MGI algorithm is used to detect hair pixels. A hair mask containing all hair pixels is shown in Fig. 2(c). The MGI algorithm uses dilation process to remove the hair pixels. The hair removal algorithm's result is presented in Fig. 2(d) where the image doesn't contain any hair pixels. Fig. 2(e) represents the enhanced image with an increase in contrast. The skin lesion is segmented using the Otsu

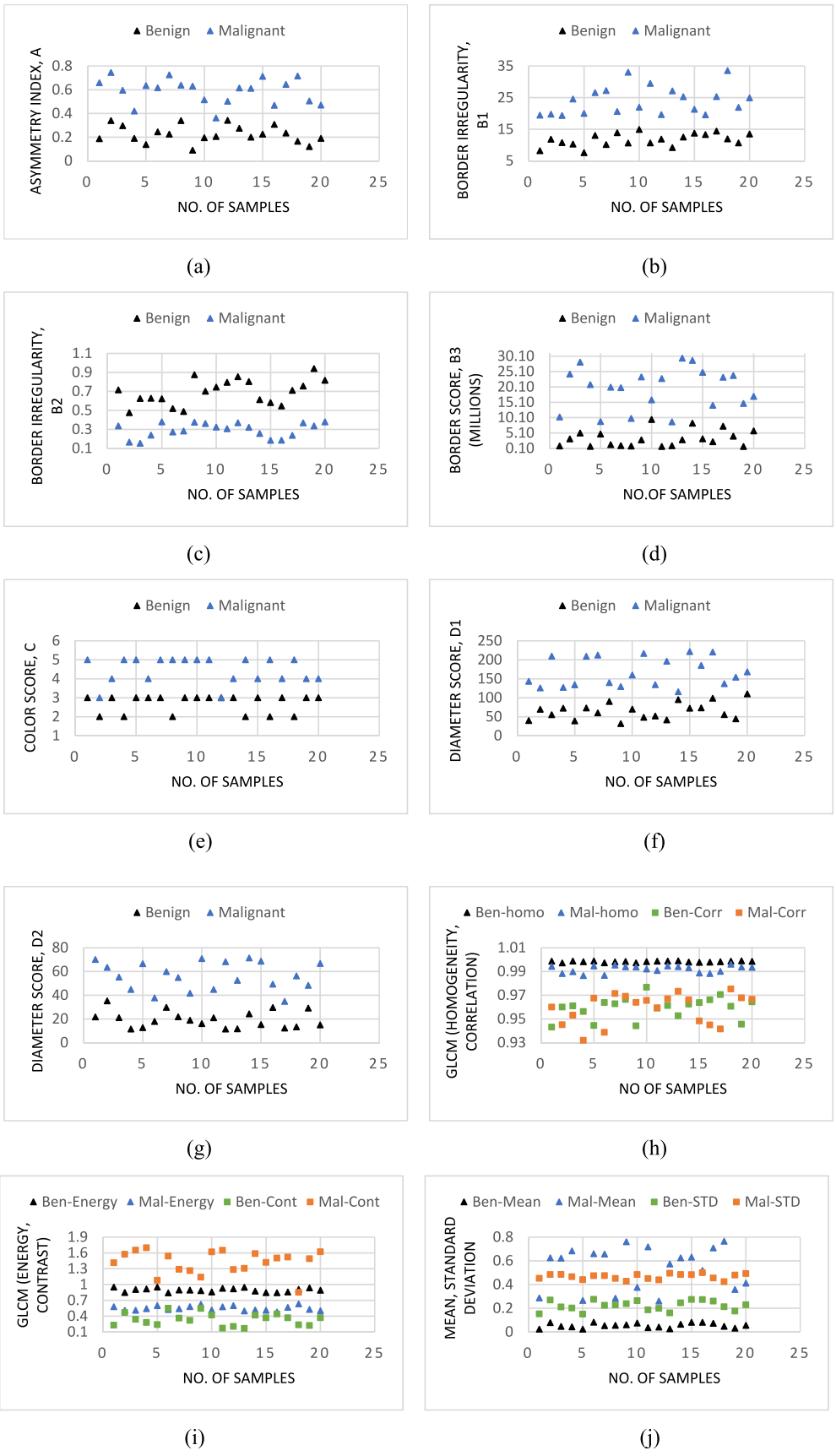

Fig. 7. (a) A score (b) B1 score (c) B2 score (d) B3 score (e) C score (f) D1 score (g) D2 score (h) Homogeneity, Correlation (i) Energy, Contrast (j) Mean, Standard Deviation for 40 images (20 benign and 20 malignant).

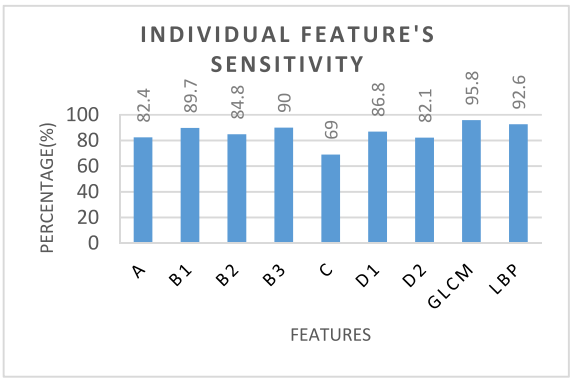

Fig. 8. Percentage of sensitivity of each feature.

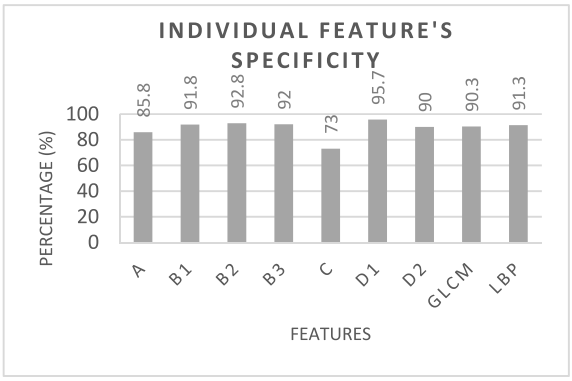

Fig. 9. Percentage of specificity of each feature.

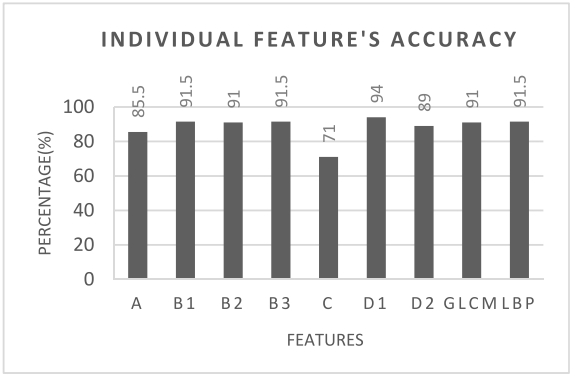

Fig. 10. Percentage of accuracy for each feature.

thresholding method and is illustrated in Fig. 2(f).

2.4. Feature extraction

Object classification is often done on the basis of characteristics of pixels inside segmented areas of interest or, (ROIs). As a result, extracting relevant features is a significant task in a successful classification process. Here the ABCD, GLCM, and local binary pattern characteristics of the skin lesion are all extracted simultaneously.

2.4.1. ABCD features

The asymmetry index (A), border irregularity (B), color score (C), and diameter (D) of the lesion are referred to as the ABCD-rule. Asymmetrical skin lesions are more likely to be malignant, whereas symmetrical lesions are more common in benign lesions. The Index of Asymmetry (AI) is determined using the following equation:

$$AI = \Delta A / A \tag{2}$$

Here, total image area is denoted by A, Δ A indicates the area of the lesion to the whole image. The border of a melanoma lesion seems to be rough, irregular, and blurred. To assess the irregularity of the border, the circularity or compactness index (B1) is determined by,

$$B1 = 4\pi A / P^2 \tag{3}$$

$$B2 = A / P \tag{4}$$

$$B3 = A^* P \tag{5}$$

This reflects lesion boundary smoothness. Since the most compact structure is a circle, compactness 1 is regarded, and compactness deviates from 1 to 0 for all other forms. The lesion of melanoma has a ragged, uneven, blurry, and erratic boundary, and hence the B1 value reaches zero [4]. B2 represents Area to Perimeter ratio and B3 represents Area and Perimeter multiplication. These features will have a larger value for malignant melanoma. Variegation in colors in dermoscopic lesions is determined using the Color feature. The amount of colors in the lesions defines the feature's score. The change in colors of lesion is another early symptom of melanoma. The malignant ones are made up of much more colors than the benign ones. The rating varies from 0 to 6, which is a ranking of 1 on each of these colors. One of the most important criteria is that a melanoma-affected mole grows larger than a regular mole. A malignant lesion is larger than 6 mm in diameter. The average diameter, D1 of the lesion is calculated by,

$$D1 = (D1' + D1'') / 2 \tag{6}$$

Where $D1' = \sqrt{(4A/\pi)}$ and $D1'' = (D + d)/2$

$$D2 = D - d \tag{7}$$

D2 represents the difference between the principal axes. D is the major axis and d is the minor axis. For Malignant melanoma, D1 and D2 will have a larger value than the benign ones.

Table 4
Comparative study with related works.

Reference	Year	Features	Accuracy
Mabrouk et al. [20]	2013	GLCM	91%
Takruri et al. [28]	2014	Wavelet features	87.1%
Codella et al. [29]	2015	Sequential Pattern Mining	93.1%
Giotis et al. [30]	2015	Color and Texture	81%
Korjakowska [21]	2016	Compactness, Color, Solidity, Dissimilarity, Symmetry, Entropy, Contrast.	93.24%
Faouzi et al. [31]	2016	LBP	76.1%
Oliveira et al. [32]	2016	ABCD (replacing D with Texture)	74%
Ihab [33]	2016	ABCD	90%
Anas et al. [34]	2017	Color and Texture	83.33%
Nidhal et al. [22]	2017	ABCD	95.45%
Alquran et al. [23]	2017	GLCM + ABCD	92.1%
Linsangan et al. [27]	2018	Asymmetry, Border, Diameter	90%
Pillay et al. [24]	2019	ABCD	75.295%
Puspitasari et al. [25]	2019	GLCM	83.86%
Nabil et al. [26]	2020	ABCD	90%
Proposed Method	2021	ABCD + GLCM + LBP	97.7%

2.4.2. Gray Level Cooccurrence matrix (GLCM) features

The GLCM approach refers to the frequency of pixel pairings in an image that have the similar gray value. To evaluate the textural characteristics of the image, the relation between both the reference pixel as well as the pixels around it is determined. For characterization of texture, it considers a set of characteristics extracted from uniform symmetrical directional GLCMs: energy, contrast, correlation, and homogeneity. Formulas for computing various GLCM functions are given in Table 1.

2.4.3. Local binary pattern (LBP) features

Local Binary Pattern is a tool used for defining a surface's texture characteristics. Texture regularity could be determined based on the LBP histogram distribution structure. Texture - based data is encoded by LBP features that are used in applications like categorization, identification. Local Binary Patterns have their origins in evaluating the structure in 2D. This algorithm's basic idea is to sum up the local characteristics of an image by contrasting individual pixel to its surroundings. As a center, a pixel is taken and a threshold value is chosen for its neighbors. Mark the central pixel with 1 if its amplitude is bigger than its relative and 0 otherwise. An LBP operator converts an image into a vector of length N that analyze the image's tiny aspects. In Table 2, for the skin lesion mentioned in Fig. 2(f), some of its features are given.

2.5. Classification

Following the extraction of the feature, the next step is to train a model from the images using these extracted features. In this work, the skin lesion identification function can be conceived as a standard binary categorization issue as there are two sorts of melanoma lesions (malignant or benign melanoma) and the objective is to allocate each skin lesion of the given dermoscopic images a suitable class label. Regarding classification, a feed-forward neural network with a backpropagation mechanism is used, where class labels are given to the ANN for learning. This is a supervised learning algorithm. The label of the target is 1 or 0, where 1 implies malignancy and 0 implies benignity. Neural networks are capable of solving issues of extreme complexity because of the capability of the neurons to process non-linearly. The Neural Network involves an input layer with the extracted features (A, B1, B2, B3, C, D1, D2, GLCM, LBP) as input neurons, an output layer and a single hidden layer containing 100 neurons. Biases and weights for small random numbers are initialized. From these values and inputs, outputs of NN prediction are determined. Differences in both the estimated value and the target value are known as an error and are reduced by continuous weight and bias updates. Levenberg-Marquardt backpropagation is set as training function. Following Levenberg-Marquardt optimization, it upgrades bias and weight values. Mean Square Error is set as a performance function. An activation function enables the model to generate complex input-output mappings for the network. Here, Tangent sigmoid function (tansig) for the hidden layer and also a linear activation function (purelin) for the final output layer is used as activation functions.

Fig. 3 illustrates the structure of the customed neural network designed for the classification of melanoma cancer. The input layer of this neural network consisting of input neurons representing the extracted features from the image, an output layer and single hidden layer of 100 neurons. The output layer gives the decision whether it is malignant skin cancer or benign skin cancer.

3. Result analysis

For image-based classification analysis, from the ISIC archive dataset and Ph2 dataset, a total of 1940 benign and 1448 malignant lesion images were taken. The proposed algorithm classified almost all the benign and malignant lesion images correctly, while it failed to detect some of the lesion images. The effectiveness of the network is evaluated using the following four criteria: accuracy, sensitivity, specificity, and precision. These parameters are calculated by,

$$Accuracy = \frac{TP + TN}{TP + TN + FP + FN} \tag{8}$$

$$Specificity = \frac{TN}{TN + FP} \tag{9}$$

$$Sensitivity = \frac{TP}{TP + FN} \tag{10}$$

$$Precision = \frac{TP}{TP + FP} \tag{11}$$

here.

TP = True Positive; stands for malignant lesions correctly identified as malignant.
TN = True Negative; determines benign lesions correctly identified as benign.
FP = False Positive; stands for malignant lesions incorrectly identified as benign.
FN = False Negative; stands for benign lesions incorrectly identified as malignant.

From the confusion matrix after training the network, the value of TP, FP, TN, FN are calculated. All of these values are given in Table 3.

So, the system results in an overall classification accuracy of 97.7% with 97.4% sensitivity, 97.9% specificity, and 97.2% precision for the image dataset. Fig. 4 shows the system's performance evaluation bar graph.

Fig. 5 shows the Mean Square Error curve. It determines the closeness of estimations to actual data. The smaller the MSE, the better is the prediction to actual. Fig. 6 depicts the ROC curve of the ANN classifier discovered throughout this experiment. The ROC space is divided by a diagonal line. Because the points are above the diagonal, it is an acceptable classification.

A further step is to analyze the responses of individual features in both malignant or benign cases. This will facilitate in understanding the effect of that feature on melanoma images. Fig. 7(a), (b), 7(c), 7(d), 7(e), 7(f), 7(g), 7(h), 7(i) and 7(j) illustrate the actual response of all features considered in benign and malignant images. For each feature, a graphical illustration of 40 images (20 benign and 20 malignant) is presented. The discrete graphs show that the less points overlapping in malignant and benign lesions, the more useful the individual feature is in melanoma cancer investigation. Almost all of the features have responded well to most of the images.

The neural network also determines the percentages of properly identified malignant lesions in comparison to all malignant lesions (sensitivity), properly categorized benign lesions in comparison to all benign lesions (specificity), and properly classified lesions in comparison to all lesions (accuracy) to every feature in Fig. 8, Fig. 9 and Fig. 10 respectively. These charts show that all of the features considered can be used to distinguish lesion images with higher accuracy, specificity, and sensitivity. As a result, the proposed features look promising and may be used clinically to diagnose melanoma cancer.

A comparative study on the basis of extraction of features and overall accuracy of different works is presented in the following Table 4. It is visible that by extracting more features from the skin lesion and when they are fed into the network, the neural network's performance increases significantly.

4. Conclusion

Melanoma, also known as malignant melanoma, is kind of a skin cancer due to unusual transformation of pigment-producing units that imparts the skin color despite the high mortality rate, most cases of initial-stage melanoma are treatable. However, even expert dermatologists find it difficult to distinguish between malignant and other benign moles in their early stages of growth. For such reason, computerized systems are being established. In this research, an effective image processing technique is suggested with ANN Classifier on the basis of hybrid texture features. Combining the features improves the accuracy of the classification results. A gradient difference-based pre-processing technique is employed to find the hair pixels in the image and then removed them. Otsu's global thresholding method is used for the segmentation and then multiple features of the lesion are obtained based on the ABCD, GLCM, and LBP feature extraction method. Target values of the input features are provided to the neural network which classifies the lesion as Benign or Malignant. This approach should increase early detection efficacy for melanoma cancer. The proposed system was analyzed on images taken from the standardized dermoscopic image database. The network has obtained 97.7% overall accuracy for the combined image. The results demonstrated that a combination of features provides more accurate results in the detection and classification of malignant and benign melanoma cancer.

Declaration of competing interest

The authors declare that they have no known competing financial interests or personal relationships that could have appeared to influence the work reported in this paper.

References

[1] Yolanda Smith, Human skin structure, SkinStruct bensouillah Ch01. https://courses.washington.edu/bioen327/Labs/Lit, 2016. (Accessed 21 February 2010) accessed.

[2] Matthew Hoffman, +Picture of the skin and skin cases. http://www.webmd.com/skin-problems-and-treatments/picture-of-the-skin#1/. (Accessed 25 November 2019) accessed.

[3] Skin Cancer Treatment (PDQ) –Health Professional Version, National Cancer Institute, https://www.cancer.gov/types/skin/hp/skin-treatment-pdq#section/all. (Accessed 5 June 2020). accessed.

[4] Sharmin Majumder, Muhammad Ahsan Ullah, Feature extraction from dermoscopy images for melanoma diagnosis, Springer Nature Switzerland AG, SN Applied Sciences 2019 (2019) 753, 1.

[5] S.M. Jaisakthi, A. Chandrabose, P. Mirunalini, Automatic skin lesion segmentation using semi-supervised learning technique. https://www.researchgate.net/publication/314948454, 2017. (Accessed 17 February 2020) accessed.

[6] Maryam Sadeghi, Towards prevention and early diagnosis of skin cancer: computer aided analysis of dermoscopy images, Ph.D. Thesis, applied science, School of Computing Science (2012).

[7] Nadia Smaoui, Souhir Bessassi, A developed system for melanoma diagnosis, International Journal of Computer Vision and Signal Processing 3 (1) (2013) 10–17.

[8] Michal Kruk, Bartosz Swiderski, Stanislaw Osowski, jaroslaw Kurek, Monika Slowinska, Irena Walecka, Melanoma recognition using extended set of descriptors and classifiers, EURASIP Journal on Image and Video Processing, 2015 (2015) 43.

[9] M. Chaithanya Krishna, S. Ranganayakulu, D.R.P. Venkatesan, Skin cancer detection and feature extraction through clustering technique, IJIRCCE 4 (2016) 3736–3742.

[10] Darshana Kokitkar, Apurva Amberkar, Vaishali Giri, Prof Krishna, Computerized automated detection of skin cancer, IJARCCE 5 (2016) 579–581.

[11] A.S. Deshpande, M. Gajbar Amruta, Automated detection of skin cancer and skin allergy, IJARCSMS 4 (2016) 248–261.

[12] H. Ganster, A. Pinz, R. Rohrer, E. Wildling, M. Binder, H. Kittler, Automated melanoma recognition, IEEE Trans. Med. Imag. 20 (Issue: 3) (2001) 233–239.

[13] J.F. Alcón, C. Ciuhu, W. Kate, A. Heinrich, N. Uzunbajakava, G. Krekels, D. Siem, G. de Haan, Automatic imaging system with decision support for inspection of pigmented skin lesions and melanoma diagnosis, IEEE J Select Top Sign Process 3 (Issue: 1) (2009) 14–25.

[14] R. Garnavi, M. Aldeen, Computer-aided diagnosis of melanoma using border- and wavelet-based texture analysis, IEEE Trans. Inf. Technol. Biomed. 16 (6) (2012) 1239–1252.

[15] S. Majumder, M.A. Ullah, Feature extraction from dermoscopy images for an effective diagnosis of melanoma skin cancer, IEEE 10th international conference on electrical and computer engineering (ICECE) (2018) 185–188.

[16] K. Kiani, A.R. Sharafat, E-shaver, An improved DullRazor for digitally removing dark and light-colored hairs in dermoscopic images, Comput. Biol. Med. 41 (Issue: 3) (2011) 139–145.

[17] T. Lee, V. Ng, R. Gallagher, et al., Dullrazor: a software approach to hair removal from images, Comput. Biol. Med. 27 (Issue: 6) (1997) 533–543.

[18] T. Mendonca, P.M. Ferreira, J.S. Marques, et al., PH2-A dermoscopic image database for research and benchmarking, 35th Annual International Conference of the IEEE Engineering in Medicine and Biology Society (EMBC) (2013) 5437–5440.

[19] Claudio Fanconi, Skin cancer: malignant vs. Benign: processed skin cancer pictures of the ISIC archive. https://www.kaggle.com/fanconic/skin-cancer-malignant-vs-benign.

[20] Mai S. Mabrouk, Mariam A. Sheha, Amr A. Sharawy, Computer aided diagnosis of melanoma skin cancer using clinical photographic images, International Journal of Computers & Technology 10 (Issue: 8) (2013) 1922–1929.

[21] J. Jaworek-korjakowska, Computer aided diagnosis of micro-malignant melanoma lesions applying support vector machines, BioMed Res. Int. 2016 (6, part 1) (2016) 1–8.

[22] K. Nidhal, EL Abbani, Zahraa, Detection and analysis of skin cancer from SkinLesions, Int. J. Appl. Eng. Res. 12 (Issue: 19) (2017) 9046–9052.

[23] Hiam Alquran, Isam Abu Qasmieh, Ali Mohammad Alqudah, Sajidah Alhammouri, Esraa Alawneh Ammar Abughazaleh, Firas Hasayen, The melanoma skin cancer detection and classification using support vector machine, in: IEEE Jordan Conference on Applied Electrical Engineering and Computing Technologies (AEECT), 2017.

[24] Verosha Pillay, Serestina Viriri, Skin cancer detection from macroscopic images, in: Conference on Information Communications Technology and Society (ICTAS), 2019.

[25] Masna Wati, Haviluddin, Novianti Puspitasari, Edy Budiman, Robbi Rahim, Firstorder feature extraction methods for image texture and melanoma skin cancer detection, J. Phys. Conf. 1230 (2019), 012013.

[26] Nadia S. Zghal, Nabil Derbel, Melanoma Skin Cancer Detection Based on Image Processing, Current Medical Imaging, vol. 16, Bentham Science Publishers, 2020, pp. 50–58. Issue: 1.

[27] Noel B. Linsangan, Jetron J. Adtoon, Jumelyn L. Torres, Geometric analysis of skin lesion for skin cancer using image processing, in: 2018 IEEE 10th International Conference on Humanoid, Nanotechnology, Information Technology, Communication and Control, Environment and Management (HNICEM), 2018.

[28] Maen Takruri, Adel Al-Jumaily, Mohamed Khaled Abu Mahmoud, Automatic recognition of melanoma using support vector machines: a study based on wavelet, curvelet and color features, Industrial Automation, Information and Communications Technology (IAICT), International Conference, IEEE, 2014, pp. 70–75.

[29] Codella Noel, Junjie Cai, Mani Abedini, Rahil Garnavi, Alan Halpern, John R. Smith, Deep learning, sparse coding, and svm for melanoma recognition in dermoscopy images, in: International Workshop on Machine Learning in Medical Imaging, Springer, 2015, pp. 118–126.

[30] G. Ioannis, M. Nynke, L. Sander, B. Michael, F. Jonkman Marcel, P. Nicolai, A computer-assisted melanoma diagnosis system using non-dermoscopic images, Expert Syst. Appl. 42 (Issue: 19) (2015) 6578–6585.

[31] Faouzi Adjed, Ibrahima Faye, Fakhreddine Ababsa, JamalGardezi Syed, Sarat Chandra Dass, Classification of Skin Cancer Images Using Local Binary Pattern and SVM Classifier, 4th International Conference on Fundamental and Applied Sciences (ICFAS), 2016.

[32] R.B. Oliveira, N. Marranghello, A.S. Pereira, J.M.R.S. Tavares, A computational approach for detecting pigmented skin lesions in macroscopic images, Expert Syst. Appl. (2016) 53–63.

[33] Ihab S. Zaqout, Diagnosis of skin lesions based on dermoscopic images using image processing techniques, International Journal of Signal Processing, Image Processing and Pattern Recognition 9 (Issue: 9) (2016) 189–204.

[34] A. Mohd, G.K. Ram, A. Shafeeq, Skin cancer classification using K-means clustering, Int. J. Tech. Res. Appl. 5 (Issue: 1) (2017) 62–65.